The Energy Spectrum of Primary Cosmic Radiation*

M. F. KAPLON, B. PETERS, H. L. REYNOLDS,† AND D. M. RITSON
University of Rochester, Rochester, New York

(Received August 27, 1951)

Techniques have been developed by which the energy spectrum of heavy primary nuclei can be measured in the energy range of 10^9–10^{11} ev/nucleon and of both protons and α-particles in the energy range from 10^{11} to 10^{13} ev/nucleon. It is shown that even the heaviest nuclei in the primary radiation ($Z\sim26$) have lost their orbital electrons before entering the atmosphere, which supports the assumption that they do nor proceed from the solar corona directly to the earth. It is also shown that the velocity spectrum of all primaries of charge $Z>1$ is independent of the mass of the nuclei, and that it differs only slightly from that of the proton component in the energy interval between 3×10^8 and 10^{10} ev/nucleon.

INTRODUCTION

PRIMARY cosmic radiation is known to consist of a mixture of nuclei whose atomic numbers range from $Z=1$ to $Z\sim26-30$.[1-4] The relative abundance of different elements in the cosmic-ray beam seems to parallel closely the relative abundance of chemical elements in the visible universe.

In order to gain further insight into the possible mechanism by which these particles may have been accelerated, it seems useful to study separately the energy spectrum of different components of the primary beam.

Data on the energy spectrum of the total primary radiation have been obtained by observing total counting rates at the top of the atmosphere.[5] Since at any given latitude over 80 percent of the primary particles are protons, these investigations yield essentially the energy spectrum of the proton component in the range between 1 and 15 Bev. Some measurements on the energy spectrum of heavier primaries have been obtained previously by measuring the flux of various components of the primary radiation at different latitudes. In Chapter I of this paper we shall present some results on the energy spectrum obtained from nuclear interactions of primary particles. The energy region covered by these measurements includes most of the latitude-sensitive part of the spectrum (<6.8 Bev/nucleon) and extends beyond it up to energies of about 50 Bev/nucleon.

These measurements together with new measurements in the nonrelativistic region of the spectrum (Chapter II) and additional flux data (Chapter III) seem to indicate that the velocity spectrum of all components of the primary beam from helium to iron is identical and can be represented by an integral spectrum of the form $N(\epsilon)=(K/(1+\epsilon)^{1.35\pm0.15})$, where ϵ is the kinetic energy per nucleon in Bev and K is a number which for each charge component is independent of energy.

Chapter IV contains a comparison of data obtained from the latitude effect with those obtained from the range and from nuclear interactions of the primary particles. This comparison provides conclusive evidence that even primary particles as heavy as iron arrive from outer space completely or very nearly completely stripped of their electronic shells. They must have lost their electrons either in the process of acceleration or in their subsequent traversal of interstellar matter. An estimate for the ionization of hydrogen-like atoms by electrons would indicate a minimum age for iron nuclei of the order of (300 years)/ρ, where ρ is the number of of protons and electrons per cc along the trajectory. This corresponds to a minimum amount of material traversed of 12 μg or about 200 times more than would be traversed by a particle proceeding directly from the solar corona to the earth.

In the course of these investigations we have obtained values for the mean-free path for nuclear collisions in brass (Chapter V) both for nuclei of charge $Z\geqslant6$ and energy above 1-Bev/nucleon and for α-particles of energy above 10 Bev. When combined with values previously obtained for the mean-free path in air and glass, it appears that the cross section for nuclei of atomic weight between helium and iron, in materials ranging in atomic weight from air to brass, can be adequately represented by the formula given previously for a more restricted range of atomic weights.[2,3]

In Chapter VI we shall briefly describe some measurements now in progress which permit determination of the flux of protons and α-particles in the energy range between 10^{11} and 10^{13} ev per nucleon. Incomplete results indicate that in this energy region the ratio of primary α-particles to protons is similar to the ratio in the latitude sensitive part of the beam.

CHAPTER I. MEASUREMENTS OF THE ENERGY OF HEAVY PRIMARIES BASED ON NUCLEAR COLLISIONS

(1) Description of the Apparatus

All the results reported in this paper are based on two high altitude flights carried out by the General

* This research was supported by the AEC.

† AEC Predoctoral Fellow, now at Oak Ridge National Laboratory, Oak Ridge, Tennessee.

[1] P. Freier *et al.*, Phys. Rev. **74**, 213 (1948).
[2] H. Bradt and B. Peters, Phys. Rev. **77**, 54 (1950).
[3] H. Bradt and B. Peters, Phys. Rev. **80**, 943 (1950).
[4] B. Peters, *Progress in Cosmic Ray Physics* (North Holland Publishing Company, Amsterdam, 1951), Vol. 1, Chap. IV.
[5] J. R. Winckler *et al.*, Phys. Rev. **79**, 656 (1950).

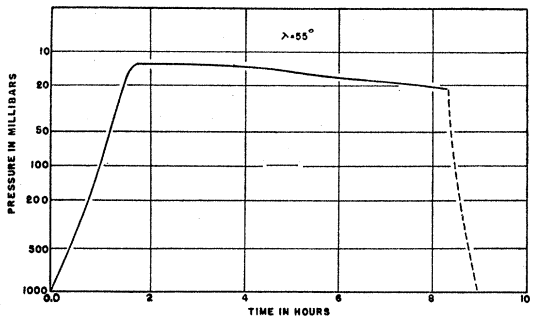

FIG. 1. Time-altitude curve for Minnesota balloon flight.

Mills Aeronautical Laboratory. One flight was made at Minnesota (geomag. latitude $\lambda=55°$) on September 24, 1950, the other at White Sands, N. M. ($\lambda=41.7°$) on February 12, 1951. Figures 1 and 2 show the time altitude curves for these flights.

In both experiments the same apparatus was used. It consisted of the box shown in Fig. 3. This box is made of 20 brass plates 3 mm thick and accurately spaced by a brass frame. Below each brass plate a nuclear G-5 emulsion of 100μ thickness mounted on a glass plate 4 in.$\times$6 in. and 1.3 mm thick was inserted. Great care was taken to insure that the plates were accurately aligned with respect to each other and evenly spaced. Six 250μ emulsions (G-5, NTB3, C2, NTA) were placed on top of the assembly. The stack was flown with the plates in a horizontal position.

(2) Collisions of Heavy Nuclei

Stars produced by energetic heavy nuclei differ in some respects from those produced by protons or α-particles. If a proton or α-particle hits a target nucleus the resulting fragmentation of the target nucleus gives rise to a variety of tracks which may roughly be classified as follows:

(a) Shower particles causing "light tracks." These consist of singly charged particles of high energy with near minimum ionization. Fowler[6] has shown that more than 75 percent of these particles are π-mesons, the remainder mostly protons. They appear only in collisions involving energies in excess of $\sim$1 Bev and increase in multiplicity as the energy increases. The tracks are usually collimated in the forward direction, the degree of collimation increasing with multiplicity.

(b) Fragments producing "grey tracks." These consist mostly of protons in the energy range from about 20 Mev to 200 Mev with a small admixture of heavier nuclei. The tracks are not collimated but are preferentially emitted in the forward hemisphere. These particles are probably the result of the nucleonic cascade started by the incident proton.

(c) Evaporation tracks consisting of about equal numbers of protons and α-particles with energies of a few Mev and some heavier fragments whose charge rarely exceeds that of a carbon nucleus. The angular distribution of these tracks is spherically symmetric.

(d) Recoil fragments. This is the part of the target nucleus which has escaped destruction in the collision and has cooled down by the evaporation of α-particles, protons and neutrons. A recoil fragment is almost always present if the target nucleus was heavy. It produces very short tracks rarely exceeding a few microns in length.

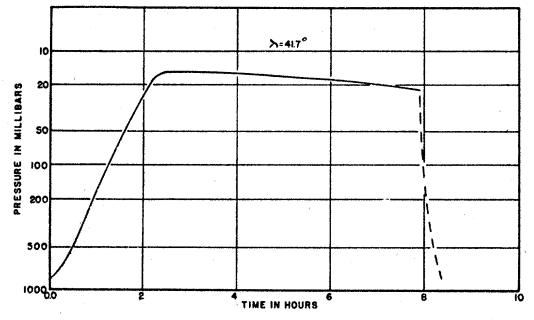

FIG. 2. Time-altitude curve for White Sands balloon flight.

If the incident nucleus is heavy, an identical set of fragments will be produced in the rest system of the projectile. The recoil fragment will in the laboratory system appear as a heavy nucleus proceeding in the direction of the incident particle with undiminished velocity. The evaporation tracks will appear as a strongly collimated beam of singly-charged and of multiply-charged particles; most of the multiply-charged particles are relativistic α-particles. These showers containing strongly collimated relativistic α-particles are characteristic of stars produced by heavy nuclei and are not observed in proton or helium produced stars. A typical event is illustrated in Fig. 4.

Perkins[7] and others have shown that α-particles ejected in the evaporation process are emitted isotropically with an average energy of 2–3 Mev per nucleon and that very rarely α-particles are emitted with more than 7.5-Mev/nucleon.

It follows that the energy and angular distribution of these α-particles in the laboratory system permit a measurement of the velocity with which the evaporating nucleus moved with respect to the laboratory frame of reference. We have obtained the energy of the incident nucleus both by measuring the angular spread of the α-particle showers and by measuring the multiple scattering of these α-particles.

(3) Energy Determination from the Opening Angle of the α-Particle Showers

For α-particles which are emitted isotropically in the rest system of the incident nucleus, the root-mean-square angle which the shower particles make in the laboratory system with the direction of motion is simply related to their mean kinetic energy in the rest system:

$$\langle\theta^2\rangle=\langle T\rangle M/3p^2. \quad (1)$$

Here $\langle T\rangle$ is the average kinetic energy of the α-particles in the rest system, M is the proton mass, and p is the momentum per nucleon of the incident particle.

Perkins[7] gives the average kinetic energy of evapora-

[6] P. H. Fowler, Phil. Mag. 41, 169 (1950).

[7] D. H. Perkins, Phil. Mag. 41, 138 (1950).

tion α-particles as 8 Mev in carbon and oxygen and as 14 Mev in silver and bromine. Since most of the particles whose energy was measured by this method belonged to the magnesium-silicon group we have chosen for $\langle T\rangle$ the value of 10 Mev. One obtains then for incident relativistic particles

$$\langle\theta^2\rangle^{\frac{1}{2}}=0.056/E, \tag{2}$$

where E is the total energy per nucleon of the incident particle in Bev. As can be seen from Eq. (1) this result is insensitive to the accurate value of $\langle T\rangle$.

If the shower contains very few α-particles, the energy estimate based on the opening angle could be quite wrong, since in the rest system all the α-particles may accidentally be emitted in the forward or backward direction or because they may all have energies well below the assumed average value of 10 Mev. Both effects would decrease the average opening angle and lead to an overestimate of the incident energy. However, as the multiplicity of the α-particles increases, the danger of a gross overestimate decreases rapidly.

If we assume that none of the α-particles can be emitted in the rest system with kinetic energies larger than 30 Mev, the largest observed angle of any shower particle will provide an upper limit for the energy of the incident particle. The largest possible angle in the laboratory system is given by

$$E\tan\theta_{\max}=\beta_{\max}(\beta^2-\beta_{\max}{}^2)^{-\frac{1}{2}}$$

or

$$\theta_{\max}\approx 0.12/\mathrm{E}. \tag{3}$$

Since $\theta_{\max}\geqslant\langle\theta^2\rangle^{\frac{1}{2}}$ it follows that the incident energy cannot be underestimated by more than a factor 2.

In order to obtain the opening angle of the α-particle showers, the following procedure was used:

(a) An area of 155 cm² of the plate on top of the "White Sands stack" was surveyed for all particles of atomic number $Z\geqslant 10$.

(b) The nuclei were identified by measuring the δ-ray density in the G-5 emulsions and the grain density in the under-developed C-2 emulsions which were placed on top of the brass stack. (See reference 3.)

(c) The tracks were followed through the brass stack until they left the stack or suffered a nuclear collision.

Of the 678 tracks found in this survey, 286 traversed the stack, 145 suffered collisions in the brass without leaving any multiply-charged particles proceeding in the original direction (A-collisions), 241 suffered collisions in which some multiply-charged fragments proceeded in the direction of the incoming track (B-collisions), and 6 stopped by ionization (see Chapter IV).

Of the 241 particles which suffered B-collisions, 77 gave rise to a shower containing at least 3 multiply-charged fast particles (mostly α-particles). We shall call these collisions "C-collisions." The energy measurements were carried out with this group. The shower was followed through additional brass plates and the position of the shower tracks was measured in successive plates.

Whenever the shower contained a fragment of charge $Z\geqslant 6$, its trajectory was assumed to define the direction of motion of the incident particle. In this case the angles

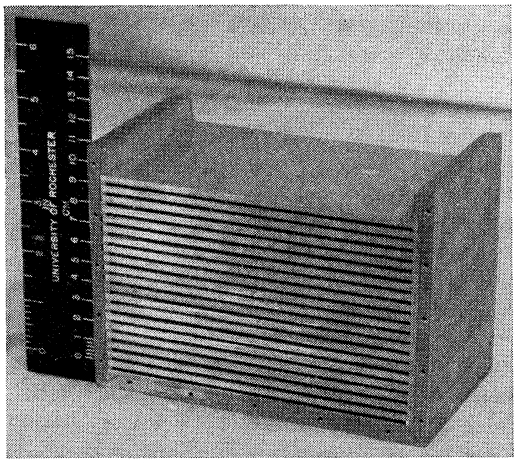

FIG. 3. Brass box used for exposing plates.

θ_i with respect to the direction of motion could be measured and the incident energy determined from Eq. (1). In most cases, however, the shower contained only α-particles and the angles ϕ_i of individual tracks were measured with respect to the center of gravity of the shower. The relation between the average value

$$\langle\phi^2\rangle=\sum_1^n\frac{\phi_i^2}{n}$$

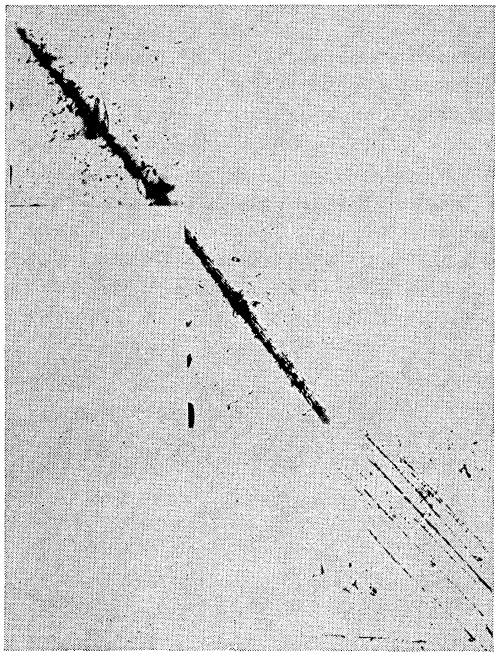

FIG. 4. C-collision: A primary Fe nucleus with a total energy of 2×10^{12} ev strikes a nucleus of the emulsion and breaks up into a highly collimated shower of 6 α-particles, a Be nucleus, and several protons. The first plate shows the incident nucleus before breakup. The second plate (4.6 mm from the first) shows the collimated shower shortly after breakup. The third plate (6.8 mm from the second) shows the separate components of the shower. The total spread in plate 3 is 30μ.

and $\langle\theta^2\rangle$ is derived in Appendix I(A) and is given by

$$\langle\phi^2\rangle=[(n-1)/n]\langle\theta^2\rangle, \tag{4}$$

where n is the number of tracks in the shower. Again the energy is obtained from Eq. (1).

Because of the finite number of particles in each shower, the energy values obtained by this method will fluctuate around the true value. By means of the Monte Carlo method we have determined the probability of obtaining a given value $\langle\phi^2\rangle$ for the average square angle of the shower particles with the center of gravity of the shower and thereby obtaining a given value ϵ' for the energy of the primary nucleus, if the true energy of the nucleus is ϵ. In Fig. 5 we have plotted the probability $P(\epsilon'/\epsilon)$ for (3- and 4-particle showers) of obtaining a value ϵ' if the true value is ϵ. The curve is based on the energy spectrum of evaporation α-particles given by Perkins.

From the mean energy $\langle T\rangle$ and the mean square energy $\langle T^2\rangle$ of Perkins' spectrum we can also calculate the mean square angle between the shower particles and the center of gravity,

$$\langle Y\rangle=\sum_i \frac{\phi_i^2}{n}=\frac{n-1}{3n}\frac{\langle T\rangle M}{p^2} \tag{5}$$

and the mean square deviation of Y:

$$\Delta^2=\langle(Y-\langle Y\rangle)^2/(\langle Y\rangle)^2\rangle=\frac{6}{5n}\frac{\langle T^2\rangle}{(\langle T\rangle)^2}-\frac{2n-3}{2n(n-1)}. \tag{6}$$

The root-mean-square error in the measured energy is approximately given by $\Delta/2$.

These calculated values are in good agreement with those obtained by the Monte Carlo method as shown in Table I.

The probability that a particle incident on a given target nucleus will make a C-collision will depend on its atomic weight and on the geometry of the collision. It is, however, reasonable to assume that it will not depend on the energy of the incident particle if this energy is very large compared to the nuclear binding energy. This follows from the model which attributes the α-particle shower to the subsequent evaporation of particles in the cooling process of the nuclear matter which has escaped disintegration in the collision. If this assumption is granted, the particles which suffer C-collisions represent a sample of the incident particles randomly selected with respect to their energy, and the energy distribution obtained represents, after correcting for the ionization loss in the residual atmosphere, the energy distribution of the incident radiation.

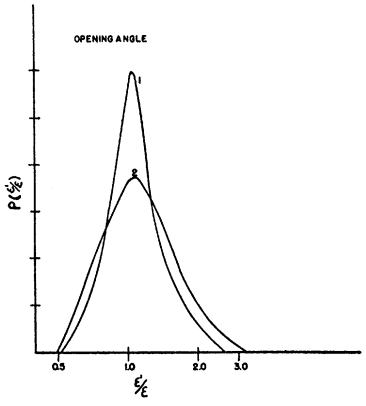

FIG. 5. Probability (in arbitrary linear units) of obtaining an energy ϵ' if the true value is ϵ for the opening angle measurements. Curves 1 and 2 are normalized to equal areas and refer repsectively to 4- and 3-particle showers.

TABLE I. Root-mean-square error, $\Delta/2$, in the measured energy.

	$\frac{\langle Y\rangle_{\text{Calc.}}}{\langle Y\rangle_{\text{M.C.}}}$	$\Delta/2$ Calc.	$\Delta/2$ M.C.
3-particle showers	0.99	0.25	0.29
4-particle showers	1.00	0.21	0.23

If the angle between the shower particles is large, the particles may already be well separated in the emulsion following the brass plate where the collision occurs, and some of the shower particles could be missed. The probability of detecting a C-collision is, however, very nearly unity if we confine ourselves to small opening angles corresponding to energies above 3.0 Bev per nucleon. This value therefore represents the lower limit for which the measurements described here can be assumed to represent the primary energy spectrum.

The upper limit for the validity of this method is determined by the smallest opening angle which can be measured. Angles of the order of 10^{-5} radian can easily be measured by measuring the separation of tracks in emulsions separated by 10 cm of brass. As shown in the next section the relative scattering of the α-particles over this distance is not large enough to affect the opening angle measurement. The upper limit therefore corresponds to an energy of $\sim$5000 Bev/nucleon.

The practical limit is slightly lower and is determined by the destruction of α-particles by nuclear collisions in the brass with a mean-free path of 9 cm. The highest energy particle actually observed in this experiment was a silicon nucleus with 45 Bev/nucleon or a total kinetic energy of 1.3×10^{12} ev.

In Fig. 6 we have plotted the number of particles whose energy exceeded ϵ Bev/nucleon *versus* ϵ. The two curves in the same graph represent the values which we would expect to find if we take into account the probability distribution of Fig. 5 and assume for the incident radiation the energy spectra indicated in the graph. Because of the reduced detection probability of C-collisions produced by low energy particles, the points below $\epsilon=3$ Bev/nucleon do not represent the true number of incident primaries and should be disregarded. Figure 6 shows that the integral energy spectrum for particles of charge $10\leqslant Z\leqslant 26$ in the energy region between $3\leqslant\epsilon\leqslant 20$ Bev/nucleon is therefore well represented by

$$N(\epsilon)=K/(1+\epsilon)^{1.35\pm0.15}. \tag{7}$$

We shall show later that the same spectrum fits the data for all primaries of charge $2 \leqslant Z \leqslant 26$ also in the region of nonrelativistic energies.

(4) Energy Determinations from the Relative Scattering of α-Particles Produced in C-Collisions

Because the α-particles forming the shower characterizing a C-collision are produced in the rest system with kinetic energies below 30 Mev or 7.5 Mev/nucleon, their total energy per nucleon in the laboratory system E_0 will very nearly be equal to that of the parent nucleus (E) if the latter is relativistic. If ϑ is the angle in the rest system between the direction of motion of the parent nucleus and the emitted α-particle, the total energy per nucleon of the α-particle in the laboratory system in units of the proton mass is given by

$$E_0 = E_0'E + [(E_0')^2 - 1]^{\frac{1}{2}}(E^2-1)^{\frac{1}{2}} \cos\vartheta. \quad (8)$$

For $E_0' < 1.008$ (corresponding to the upper limit of 30 Mev for the α-particle energy in the rest system) we get

$$(|E_0 - E|)/E \leqslant 13 \text{ percent}. \quad (9)$$

We therefore obtain a nearly monoenergetic beam of α-particles whose average enery per nucleon is equal to that of the incident particle. The energy of the incident nucleus can therefore be determined by measuring the energy of the α-particles in the laboratory system.

The determination of particle energies from multiple coulomb scattering in emulsion has been described by several authors.[8,9] The method as previously applied is limited to energies below a few Bev per nucleon. In order to make measurements in the energy range between 1 and 100 Bev/nucleon it is necessary to reduce the reading error by using larger cell lengths than those available for tracks in a single emulsion and to avoid errors arising from the distortion of the emulsion and from inaccuracies of the microscopic stage.

The first can be accomplished in our arrangement by measuring the position of the track in different emulsions separated by several millimeters of absorber and by tracing the shower through distances of 10–20 cm.

Inaccuracies of the stage motion are eliminated by measuring only the relative scattering of the particles, i.e., measuring the relative separation of the shower tracks in successive plates.

The effect of distortions in the emulsion can be avoided by measuring the distances between tracks at the point where they enter the glass of the plate. The accurate location of the entrance point was facilitated in our experiment:

(a) by using emulsions of high sensitivity (the grain density for a relativistic α-particle was >130 g/100μ).

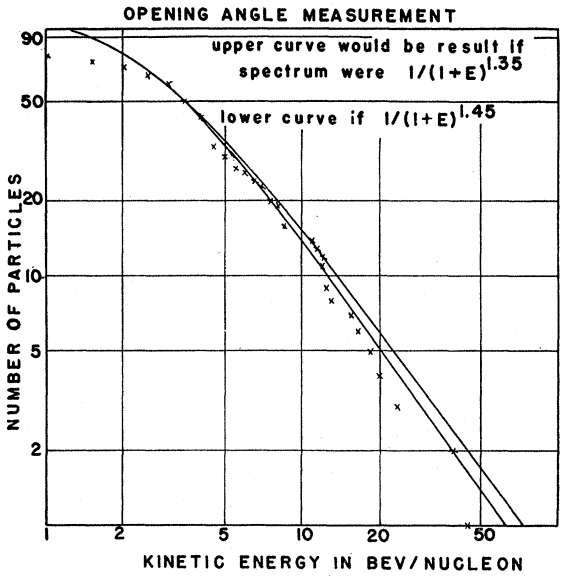

FIG. 6. Integral energy spectrum obtained from opening angle measurements.

(b) by using thin emulsions (100μ) which will not peel even if the usual coating between emulsion and glass is omitted,

(c) by using plates in a horizontal position such that most tracks are steeply dipping.

If X, X', X'' are the x or y coordinates of a given track at successive intervals of length t, the scattering S is defined by $S = X + X'' - 2X'$ and the energy is related to the average value of S^2 by

$$(\langle S^2 \rangle)^{\frac{1}{2}} = (Kt^{\frac{3}{2}})/p\beta, \quad (10)$$

where p, β are the momentum per nucleon and the velocity of the α-particle. For scattering in emulsions the constant K has been evaluated by Gottstein *et al.*[10] and agrees with the value calculated from a formula given by Williams.[11]

The value of K for the mixture of brass, glass, and emulsion used in our experiment is calculated in Appendix II.

Since in our experiment the coordinates of the track are measured not with respect to a straight line of reference, but with respect to the line connecting the centers of gravity of the shower in successive plates, our measurements yield a quantity $\langle S^2 \rangle$ which is related to the true scattering by the relation derived in Appendix I(B)

$$(\langle S^2 \rangle)^{\frac{1}{2}} = [(n-1)/n]^{\frac{1}{2}}[\langle (S^T)^2 \rangle]^{\frac{1}{2}},$$

where n is the number of tracks in the shower. In our method of determining the scattering S, we have eliminated errors which arise from inaccuracies of the microscope stage and distortion of the emulsion. Our main error comes in determining the point where the track enters the plane of the glass, because of the finite

[8] P. Fowler, Phil. Mag. **41**, 169 (1950).
[9] Y. Goldschmidt-Clermont, Nuovo cimento **7**, 1 (1950).
[10] K. Gottstein *et al.*, Phil. Mag. **42**, 708 (1951).
[11] E. J. Williams, Phys. Rev. **58**, 292 (1940).

size of grains and possible inhomogeneities of the glass surface.

A number of errors in the determination of S arise also from possible misalignment of successive plates. These are: (a) rotation, (b) tilt, and (c) unequal plate spacing.

(a) By comparing the position of tracks of heavy nuclei penetrating opposite corners of the stack, it was established that relative rotation is less than 1/300 of a radian. Since no measurements were made on showers when the distance of any track from the center of gravity of the shower exceeded 600μ, and since for showers of energy above 5 Bev/nucleon the distance did not exceed 300μ, this correction amounts only to a few percent of the scattering and can be neglected.

(b) The relative tilt of successive plates which was measured to be less than 1/500 of a radian has still less influence on the measurements since the errors produced by tilt are proportional to the tangent of the zenith angle under which the track enters, and this angle was almost always much less than 45°.

(c) The errors produced by unequal plate spacing are more serious. They produce variations of the distance of the track from the center of gravity of the shower which are proportional to the opening angle and therefore inversely proportional to the particle energy. Since the scattering is also inversely proportional to the energy, the spurious scattering due to variation of plate spacing produces a percentage error in the scattering measurements which is the same for showers of any energy. The variation of individual plate spacing amounted to about 0.1 mm or 2 percent of the average plate spacing of 5 mm. Over the distance of one plate spacing the spurious scattering amounts therefore to about 40 percent of the true scattering. Since this number is independent of the energy of the shower and since errors must be added in a Gaussian manner, the error introduced is not too serious. Fortunately, however, it can be eliminated. The spurious scattering produced by errors in plate spacing increases or decreases the separation of tracks from the center of gravity by the same percentage, while the true scattering changes these distances in a random manner. Consequently the error introduced by variation in plate spacing can be eliminated in the statistical treatment of the data. This is done in Appendix IC.

Our total spurious scattering resulting from noise was determined to be $\sim 1\mu$.

The probability $P(\epsilon'/\epsilon)$ of obtaining from the scattering measurements an energy value ϵ' if the true energy is ϵ, has been calculated on the basis of an assumed gaussian distribution in S, leading to a Γ-distribution in $\langle S^2 \rangle$. The resulting probability distribution is shown in Fig. 7. The results of the scattering measurements have been plotted in Fig. 8, where they can be compared with the curves which give the results to be expected from these measurements if the true energy distribution of the particles at the top of the atmosphere followed the distribution laws indicated in the graph.

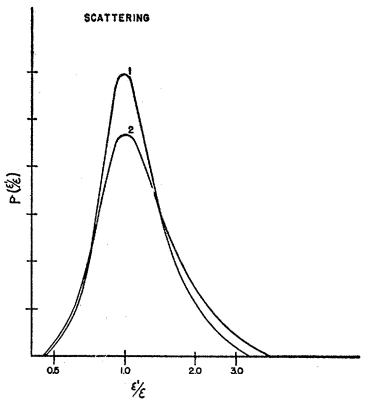

FIG. 7. Probability (in arbitrary linear units) of obtaining an energy ϵ' if the true value is ϵ for the scattering measurements. Curves 1 and 2 are normalized to equal areas and refer, respectively, to 6 and 4 independent readings.

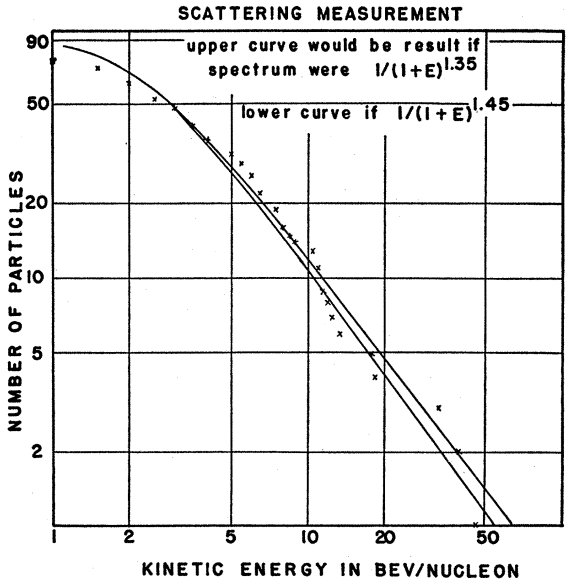

FIG. 8. Integral energy spectrum obtained from scattering measurements.

The two independent methods by which the energy of particles producing C-collisions is obtained not only give the same energy spectrum, they also give particle energies which in almost all cases are in good agreement with each other. We have calculated on the basis of the probability distributions shown in Figs. 5 and 7 the expected distribution in the ratio of energy values determined by the two methods. Figure 9 shows the expected and observed ratios and indicates that the results obtained by the two methods are consistent with each other.

Table II lists a random sample of events:

(a) The first column identifies the primary nucleus.

(b) The second column lists the particles of charge $Z>1$ in the shower.

(c) The third column gives the cell length used for the scattering measurements.

(d) The fourth column gives the number of independent scattering measurements made. This number is $(2n-3)(c-1)$ where c is the number of cells and n the number of shower particles. The number 2 is due to the fact that scattering is measured in two mutually perpendicular directions. The factor $c-1$ appears because 2 cells are required to establish second differences. The number 3 in the bracket arises because in each measurement two readings are required to refer the scattering to the center of gravity of the shower and one reading to correct for errors in plate spacing.

(e) The fifth and sixth columns give the energy values obtained from scattering and mean square opening angle, respectively.

(f) The last column is an upper limit on the energy of the particle

derived from the largest angle in the shower as explained in Chapter I, (3).

The method of measuring the energy of primary particles outlined in this chapter is limited to particles of charge $Z \geqslant 10$ because only very heavy nuclei produce showers with 3 or more α-particles with appreciable probability. The interpretation of the results in terms of a primary energy spectrum is further dependent on the assumption discussed in I, (3), that the probability of C-collisions is independent of the particle energy at high energies. This assumption, while very reasonable, cannot as yet be proved; however, even a variation of this probability of as high as 20 percent in the energy range from 3–10-Bev/nucleon would not affect our results within the statistical error. In Chapter V it is shown that the interaction cross section of heavy nuclei does not strongly depend on energy.

It may be possible to overcome these limitations at least partially by using absorbers rich in hydrogen instead of brass between the emulsions. The probability that a collision between a very heavy nucleus and a proton results in a measurable shower may then approach unity and may be appreciable even for primaries of the carbon, nitrogen, oxygen group.

Another possible method of extending these techniques, however, consists in measuring the scattering of single unrelated tracks with respect to the track of a particle of very high energy. In Chapter VI it is shown that particles with energies between 10^{11} and 10^{13} ev can easily be found and identified in our brass stack and can therefore be used as a reference line for scattering measurements on any other penetrating particle.

For the purpose of carrying out measurements described in this section, Bausch and Lomb Optical Company have constructed a special microscope according to our specifications. This microscope possesses an accurate screw by which the plate, rotated through an arbitrary angle, can be moved over long distances which are easily measurable with an accuracy of 0.2μ.

CHAPTER II. THE NONRELATIVISTIC PART OF THE SPECTRUM FOR PRIMARY COSMIC-RAY PARTICLES OF CHARGE $Z \geqslant 6$

The energy of heavy nuclei below 1 Bev/nucleon can be determined by measuring their range in an absorber; these nuclei have an appreciable chance of slowing down and coming to rest because of the high ionization loss of multiply charged particles. Tracks of particles which are slowing down show an appreciable increase in δ-ray density or grain density along their trajectory, and can be identified by methods previously described.[1,2] For determining the range and thereby the energy spectrum of heavy nuclei we have used the brass stack flown at geomagnetic latitude $\lambda = 55°$ described in Chapter I. This stack is well suited for such measurements because a particle entering from the vertical has to traverse 60 g/cm² of brass and glass before leaving the stack and its

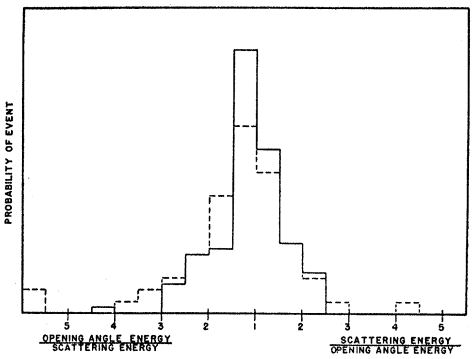

FIG. 9. Probability (in arbitrary linear units) of obtaining a given ratio for the energies as determined by opening angle and scattering measurements (the larger energy has been taken as the numerator). The dotted lines indicate the observed results and are normalized to the same area as the calculated values.

δ-ray density can be observed at intervals of 5 mm corresponding to 3 g/cm².

By limiting our investigation to those tracks which entered in a direction presenting at least 60 g/cm² of absorbing material to the particle, we did not bias our selection as far as particle energy is concerned because at that latitude the primary flux is known to be isotropic in zenith angle.[2]

At the latitude of Minnesota the earth's magnetic field permits the entry of particles of $Z>1$ if their energy exceeds 0.3 to 0.35 Bev per nucleon. However at the altitude at which our experiment was carried out ($\sim$20 g/cm² of residual atmosphere), particles whose energy was close to the cut-off value could reach the stack only if their atomic number was below that of neon. Our experiments therefore yield an energy spectrum for the CNO group for energies $\epsilon > 0.35$ Bev/nucleon and for heavier particles for energies $\epsilon \gtrsim 0.55$ Bev/nucleon.

Particles found in a survey of the top emulsion were followed through the stack until they either had

TABLE II. Energy of heavy primary nuclei determined from their breakup products.[a]

Primary	Shower particles	Cell length mm	Number of independent readings	Energy from scattering Bev/nuc.	Energy from opening angle Bev/nuc.	Upper limit of energy from opening angle Bev/nuc.
Fe^{26}	$Be^{4}+6\alpha$	27.0	17	32.5	23.0	37.0
Na^{11}	4α	13.7	5	4.7	4.8	10.0
Mg^{12}	4α	5.2	5	3.9	3.6	8.0
Ca^{20}	$B^{5}+4\alpha$	6.0	7	1.95	1.9	3.5
Si^{14}	$Ne^{10}+2\alpha$	5.1	9	1.3	2.1	4.5
Si^{14}	$Li^{3}+3\alpha$	11.1	8	11.1	11.2	22.0
Al^{13}	3α	10.3	12	7.4	7.8	16.8
Mg^{12}	4α	6.5	5	1.5	1.5	2.8
Al^{13}	4α	5.4	5	0.64	0.56	1.5
Si^{14}	4α	16.0	3	46.0	44.0	75.0
S^{16}	$F^{9}+2\alpha$	6.2	9	5.0	3.7	6.8
Fe^{26}	$O^{8}+3\alpha$	6.4	5	0.36	0.69	1.7

[a] The range of the O^{8} fragment in the last shower indicates the energy lies between 0.37 and 0.42 Bev per nucleon.

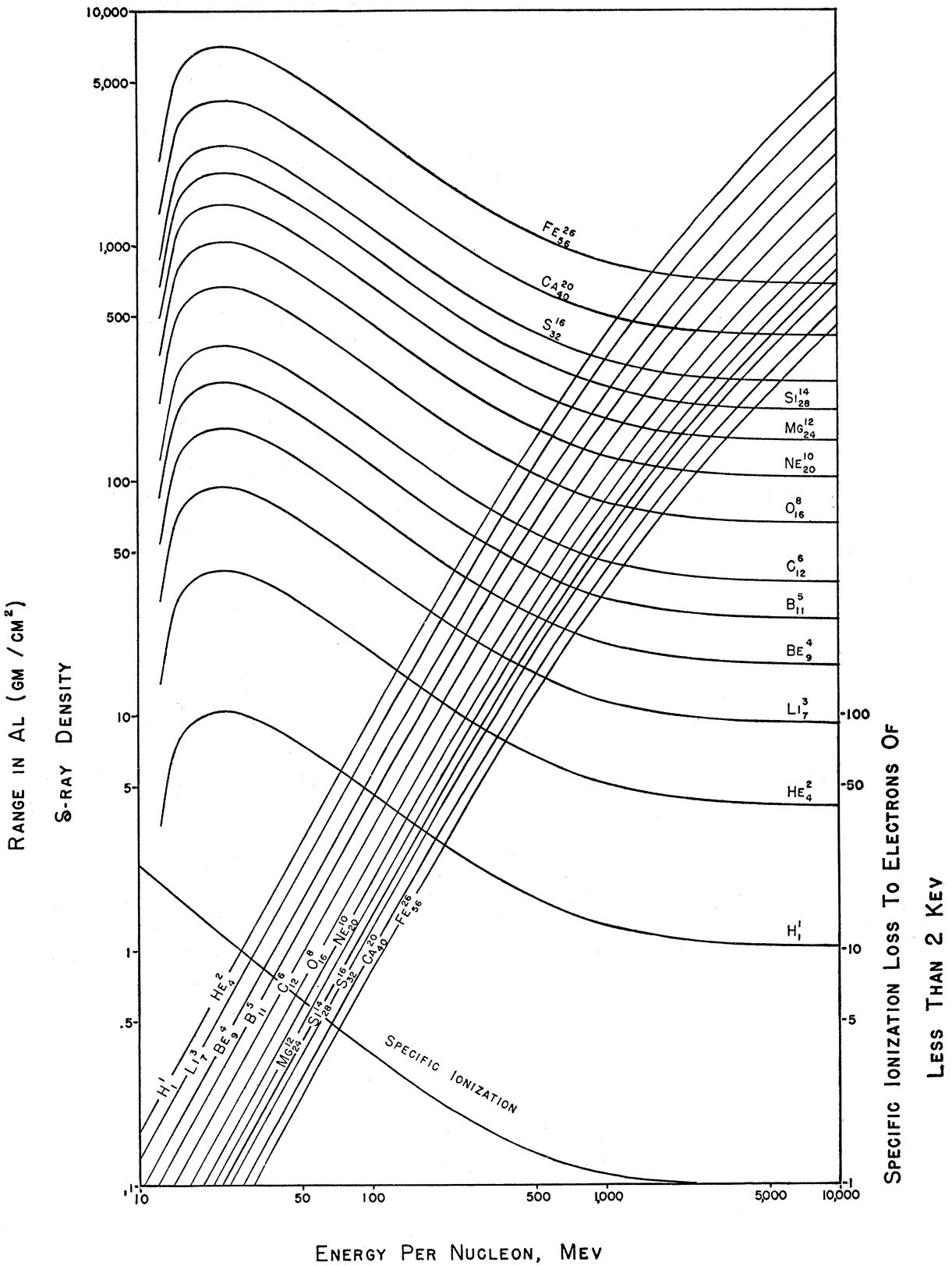

FIG. 10. Range, δ-ray density, and specific ionization loss to electrons of less than two kev as a function of energy in Bev per nucleon for various nuclei.

traversed 60 g/cm² or had disappeared in the brass plate between two emulsions. If the track showed a consistent increase in δ-ray density in the plates preceeding its termination it was classed as a particle of an ionization range determined by the length of its trajectory from the top of the atmosphere to its end point. If the particle did not change its δ-ray density it was classed as a particle which had suffered a nuclear collision.

The uncertainty in the measured range of stopping particles is of the order of the thickness of the brass absorbers (3 g/cm²) and, being only a small fraction of the total range from the top of the atmosphere, produces only a small error in the range spectrum.

The range-energy relation for particles of different charge and mass are known since they are simply derived from the range-energy relation for protons

$$R(Z, M, \epsilon)=(M/Z^2)R(1, 1, \epsilon),$$

where ϵ is the energy per nucleon. Figure 10 shows the dependence of R on ϵ for particles of different atomic numbers. The greatest uncertainty in converting our range spectrum into an energy spectrum arises from errors in the charge determination. The charge was determined with the help of the sensitive and insensitive emulsions (see Appendix III) on the top of the stack by methods previously described.[3,12] However, since in this experiment horizontal plates were used and therefore the tracks investigated were steeply dipping and short, the error in charge determination is greater than in previous experiments and probably as large as 20–25 percent. This fact and the limited number of tracks investigated restrict us to establishing an energy spectrum for two groups of primary nuclei:

$$6\leqslant Z\leqslant 9 \quad \text{and} \quad Z\geqslant 10.$$

In reducing the observed range spectrum to an energy spectrum of particles at the top of the atmosphere, we also have to make a correction for those particles which suffered nuclear collisions before they came close to the end of their range. This correction was made on the assumption that for particles of energy $0.35<\epsilon<1.5$-Bev/nucleon the cross section for nuclear collision is independent of energy. However, even if the nuclear cross section should vary by as much as 50 percent in this energy interval, the spectrum obtained from the range data would hardly be affected.

An area of 12.5 cm² was surveyed for primaries of the CNO group. We found a total of 136 particles of which 33 traversed the stack, 70 suffered nuclear collisions, and 33 came to the end of their range. A similar survey in an area of 29 cm² for particles of charge $Z\geqslant 10$ yielded 77 particles of which 12 traversed the stack, 43 suffered nuclear collisions, and 22 came to the end of their range. It was found that of the particles whose range exceeded R g/cm² the fraction of particles coming to rest in the interval between R and $(R+10)$ g/cm² was: 7.8±1.4 percent for the CNO group and 9.4±2.4 percent for the $Z\geqslant 10$ group in the range interval $27<R<80$ g/cm². Figure 11 shows the integral energy spectrum obtained from these measurements, as well as flux values obtained at geomagnetic latitudes $\lambda=55°$ and $\lambda=41.7°$.

The low energy data can be represented by an integral spectrum:

$$N(\epsilon)=K/(\alpha+\epsilon)^{1.35},$$

where $\alpha=0.9\pm0.2$ for the CNO group, $\alpha=1.0\pm0.3$ for $Z\geqslant 10$, and ϵ is the kinetic energy in Bev/nucleon. This is in agreement with the empirical spectrum derived for the high energy region.

CHAPTER III. THE DETERMINATION OF THE ABSOLUTE INTENSITY OF DIFFERENT COMPONENTS OF PRIMARY RADIATION

The survey of the plates on top of the brass stacks flown at geomagnetic latitude $\lambda=41.7°$ and $\lambda=55°$ can also be used to obtain the flux of heavy nuclei at these latitudes. The necessary corrections for nuclear absorption have been described previously.[2] A charge calibration for the tracks was achieved by comparing their δ-day density with that of α-particles in the sensitive emulsions and their grain density with that of slow α-particles in the insensitive emulsions (see reference 3 and Appendix III). At $\lambda=41.7°$ (cut-off energy 1.5 Bev per nucleon) the particles enter the stack with relativistic velocity. The δ-ray density for relativistic carbon tracks was found to be 3.7 δ-rays per 100μ.

(1) Flux at Geomagnetic Latitude $\lambda=41.7°$

The survey of the top emulsion was carried out in such a way as to include all particles whose δ-ray density exceeded 2.5 δ-rays/100μ. In 12.25 cm² we

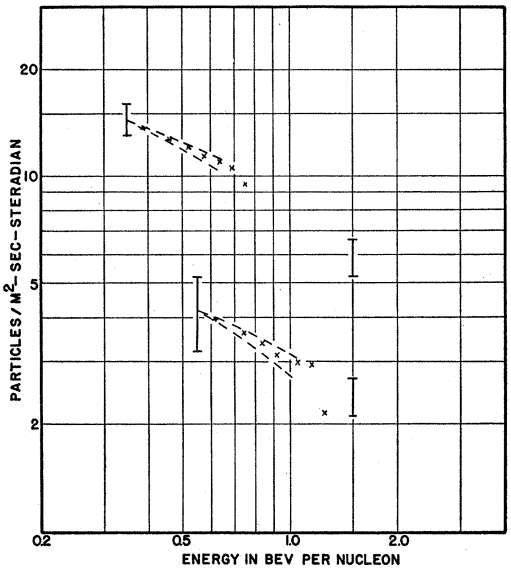

FIG. 11. Integral energy spectrum obtained from range measurement. The dotted lines refer to the errors quoted in the text.

[12] H. Bradt and B. Peters, Phys. Rev. 74, 1828 (1948).

found 100 particles which penetrated at least 8 g/cm² of absorber. This survey should therefore include all particles of charge $Z \geqslant 6$. In order to test this point an additional area of 1 cm² was surveyed to include all tracks whose δ-ray density exceeded 1.7 δ-rays per 100μ. Fifty-one additional tracks were recorded but none of them penetrated 8 g/cm² of absorber, proving that these tracks were caused by slow secondary singly or doubly charged particles.

It also suggests that primary nuclei of beryllium or boron with an energy above 1.5 Bev/nucleon are rare or absent at this latitude. This is in agreement with our previous result at $\lambda=30°$ [3] but in disagreement with the result obtained by Dainton *et al.*[13] at $\lambda=54°$.

The flux of primaries at $\lambda=41.7°$ was determined as $I(41.7°)=5.9\pm0.7$ particles/m² sec steradian for $6\leqslant Z \leqslant 9$ and $I(41.7°)=2.4\pm0.3$ particles/m² sec steradian for $Z\geqslant 10$.

The errors given are the statistical standard deviation. The upper value is in very good agreement with results recently obtained by Van Allen[14] at the same latitude with an ionization chamber mounted on a rocket. The value for particles of charge $Z\geqslant 10$ is twice as high as Van Allen's value.

(2) The Flux at Geomagnetic Latitude $\lambda=55°$

In order to obtain from the number of tracks observed to enter the stack at $\lambda=55°$ the flux of particles at the top of the atmosphere, it is necessary to correct not only for particles lost by nuclear collisions in the residual atmosphere, but also for those particles which when arriving at large zenith angles have not sufficient range to reach the stack. Since the range spectrum has been determined (Chapter II), this correction can be made down to energies determined by the atmospheric cutoff for vertical incidence. This atmospheric cut-off value is lower than the geomagnetic cut-off value for particles of charge $Z<10$ and therefore the flux obtained for the CNO group includes presumably all particles entering at that latitude (see Chapter IV). For heavier particles the atmospheric lies above the geomagnetic cutoff; our flux values therefore refer only to particles with energies above 0.55 Bev/nucleon. Additional particles presumably arrive at this latitude with energies between 0.35 and 0.55 Bev/nucleon and are stopped by the residual atmosphere. The flux values at this latitude were determined as: $I(55°)=14.4\pm1.4$ particles/m² sec steradian for CNO ($\epsilon\geqslant 0.35$ Bev) and $I(55°)=4.2\pm1.0$ particles/m² sec steradian for $Z>10$ ($\epsilon\geqslant 0.55$ Bev). Within experimental error these values agree with previous determinations at this latitude.[3,4]

CHAPTER IV. THE ENERGY SPECTRUM OF PRIMARY COSMIC-RAY PARTICLES

Before the latitude effect, which has been observed both in the total radiation (mostly protons) and in the heavy component, can be interpreted in terms of an energy spectrum, it is necessary to consider two problems:

(a) The determination of the number of primary protons entering the atmosphere is complicated by the fact that they cannot easily be distinguished from secondary high energy protons produced in collisions in the upper atmosphere. This difficulty is not eliminated if the flux is measured outside the atmosphere by telescopes carried in rockets. Secondary protons are leaving the atmosphere and may even return again after being bent back by the earth's magnetic field at large distances. That this effect is appreciable was shown by Van Allen,[15] who obtained at a height of about 100 km a counting rate which increased strongly with zenith angle. The observed angular distribution $I(\theta°)=I(0°)(1+0.6\sin\theta)$ was interpreted as due to an appreciable atmospheric albedo, which may be expected to increase with zenith angle. The values for the total primary flux collected by Winckler *et al.*[5] represent therefore still an upper limit to the true flux.

Apart from its effect on the absolute flux value, the albedo may also produce a distortion of the energy spectrum since it may be expected that the more energetic primaries give a larger contribution to the albedo than primaries of low energy. In this case the total counting rate at the top of the atmosphere will fall off more slowly with latitude than the primary intensity. For this reason, the exponent in the energy spectrum given by Winckler *et al.*, which refers mainly to the proton component and can be represented by $N(\epsilon)=K/(1+\epsilon)^{1.07}$ may be too low.

(b) The difficulty which arises in the determination of the primary proton flux does not arise in determining the flux of heavy primaries. Collisions in the upper atmosphere will either destroy the particle completely or result in some heavy fragments which will proceed undeviated in the original direction and cannot leave the atmosphere.

However, in trying to convert the latitude effect for heavy primaries into an energy spectrum we encounter another problem: we must know the charge to mass ratio of these nuclei at the time they enter the influence of the earth's magnetic field, i.e., far outside the atmosphere.

We propose to show that even the heaviest nuclei observed in the primary beam ($Z\sim 26$) are completely stripped of electrons when they come under the influence of the earth's magnetic field, and that therefore their charge to mass ratio is known to have the value $Z/M\approx\frac{1}{2}$.

Some indication of this can already be obtained from the fact that the direct energy measurements described in Chapters I and II agree with the spectrum which one obtains from the latitude effect if one assumes that the nuclei arrive completely stripped of electrons.

[13] A. D. Dainton *et al.*, Phil. Mag. **42**, 317 (1951).
[14] J. A. Van Allen, private communication.
[15] J. A. Van Allen and A. V. Gangnes, Phys. Rev. **78**, 50 (1950).

TABLE III. Cut-off data for particles at geomagnetic latitude $\lambda=41.7°$.

	Cut-off energy in Bev/nuc. completely stripped	Range in g/cm² Al	Cut-off energy in Bev/nuc. with K-shell present	Range in g/cm² Al	Cut-off energy in Bev/nuc. with K and L shell present	Range in g/cm² Al
Fe	1.35	49.6	1.21	43.0	0.655	18.2
Ca	1.50	69.0	1.29	58.0	0.525	16.0
Si	1.50	98.6	1.21	65.6	0.20	4.7
Mg	1.50	115.	1.16	83.4	0.07	0.87
Ne	1.50	138.	1.09	92.0	0	0

An investigation whether or not very heavy nuclei appear in the cosmic radiation with energies below the geomagnetic cutoff calculated for particles of $Z/M=\frac{1}{2}$ cannot easily be carried out at northern latitudes because it requires exposure of plates at altitudes not yet accessible to balloons. At $\lambda=41.7°$, however, such an investigation is possible.

We have two identical brass stacks which were flown under nearly identical conditions at $\lambda=55°$ and $\lambda=41.7°$. Since as described in Chapter II we know the intensity of the low energy component at $\lambda=55°$, we can calculate how much of this component would have been excluded at $\lambda=41.7°$ if the particles entered the earth's field: (α) completely stripped of electrons, (β) retaining only the K shell, and (γ) retaining both the K and L shells. From this we can calculate how many of the particles should have come to the end of their range and stopped in the White Sands stack under each of the foregoing assumptions and compare it with the actual number of stopping tracks observed.

Table III shows the cut-off energy and cut-off range for different nuclei at $\lambda=41.7°$ under the three different assumptions given above. Table IV shows the number and type of nuclei which came to the end of their range in the White Sands stack as well as the number expected under the three different assumptions. As can be seen from Table IV the heavy nuclei arrive either completely stripped or retain at most one or two electrons.

If we make the assumption that heavy nuclei are only partially ionized at the source of cosmic radiation, as seems to be the case for all regions of the universe accessible to spectral analysis, we obtain a lower limit for the amount of matter which the particles must have traversed before approaching the earth. Making use of calculations given by Williams,[16] the cross section for the loss of an electron from the L shell of iron due to the passage of a proton or electron is

$$\sigma=4.7\times10^{-22}\text{ cm}^2\text{ for }\beta=1.$$

It rises to a maximum:

$$\sigma=2\times10^{-19}\text{ cm}^2\text{ for }\beta=4.8\times10^{-2}$$

and from there it drops rapidly as the velocities decrease further. At the most favorable velocity an iron ion must therefore traverse at least 12μ g/cm² of ionized hydrogen gas in order to lose most of its L electrons and more if the intervening material is not ionized. This according to Van de Hulst[17] represents nearly 200 times as much material as the particle would encounter if travelling directly from the solar corona to the earth. The direct passage of heavy primaries from the solar corona to the earth seems, therefore, to be excluded.

Having established that heavy nuclei are completely stripped of electrons before approaching the earth we can now use the flux data at different latitudes in conjunction with information obtained from nuclear collisions (Chapter I) and range distribution (Chapter II) to construct the integral energy spectrum of primary cosmic radiation. The spectrum is shown in Fig. 12. The vertical bars represent flux measurements[18] corrected to the top of the atmosphere on the assumption of an incident isotropic radiation.[2] The dots and crosses represent the results obtained from opening angles and relative scattering of particles in α-particle showers normalized to the flux measurements at 3 Bev. In the helium spectrum we have used the values obtained with counters by Ney[19] at $\lambda=55°$ and Perlow[20] at $\lambda=41°$ as well as our own earlier measurements at $\lambda=51°$ and 30°.[2,4]

The proton spectrum is obtained from the spectrum given by Winckler[5] after subtracting the contribution of the heavy component. The total number of nucleons incident on the top of the atmosphere as a function of energy is also shown in the graph. The curves drawn for the heavy nuclei represent the spectrum

$$N(\epsilon)=K/(1+\epsilon)^{1.35},$$

where ϵ is the kinetic energy per nucleon in Bev and K has the values $K=400$ particles/m² sec steradian for helium, $K=20$ particles/m² sec steradian for the CNO group, and $K=8$ particles/m² sec steradian for $Z\geqslant10$.

The latitude effect for primaries in the last two groups

TABLE IV. Particles stopping in stack.

	1 No. of particles which should be seen stopping if all are stripped	No. observed stopping	2 No. of particles which should be seen stopping if they had retained K-shells	3 No. of particles which should be seen stopping if they had retained K- and L-shells	No. observed below cut-off for completely stripped particles
Fe	3.8	3	5.4	17	0
Ca	1.5	1	2.8	13	0
Si	0.6	2	4.4	53	0
Mg	0	0	2.3	65	0
Total	5.9	6	14.9	148	0

[16] E. J. Williams, Kgl. Kanske Videnskab. Selskab, Mat.-fys. Medd. XIII, 4 (1935).

[17] H. C. Van de Hulst, Astrophys. J. **105**, 471 (1947).

[18] The experimental point for the CNO group at $\lambda=0°$ represents preliminary unpublished data obtained from equatorial flights carried out in India by B. Peters *et al.* in October, 1950.

[19] E. P. Ney and D. M. Thon, Phys. Rev. **81**, 1068 (1951).

[20] G. J. Perlow and L. R. Davis, private communication.

has also been measured by Ney *et al.*[21] Their results are in agreement with ours within the experimental error.

The energy distribution in Fig. 12 is, however, in disagreement with that reported by Dainton *et al.*,[13] who measured the energy spectrum of heavy nuclei incident at $\lambda=54°$ by multiple Coulomb scattering of tracks in single emulsions. Their latest data[22] suggest that only 28 percent of the particles incident at this latitude have energies above 1.5 Bev per nucleon and only 8 percent energies above 3.5 Bev/nucleon. The corresponding calues in our spectrum are 45 percent and 21 percent, respectively. It is difficult to see how the resuls of these authors can be reconciled with the observed intensity ratio of 4–5 between $\lambda=54°$ (cut-off energy 0.4 Bev/nucleon) and $\lambda=30°$ (cut-off energy 3.5 Bev/nucleon).

The proton spectrum in Fig. 12 can be represented by the formula

$$N(\epsilon)=4000/(1+\epsilon)^{1.07} \text{ particles/m}^2 \text{ sec steradian.}$$

As explained in the beginning of this section, the true exponent may be slightly higher and the numerator slightly lower, since the flux measurements include some secondary particles.

In any case, it seems that the velocity spectrum of all particles of charge $Z>1$ is independent of the mass of the particle and that the chemical composition of that part of the beam stays constant for energies between $0.35<\epsilon\lesssim 10$ Bev/nucleon.

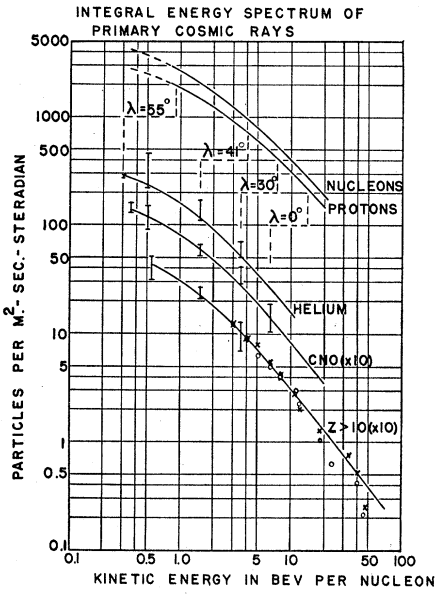

FIG. 12. Integral energy spectrum of primary cosmic radiation. The vertical bars represent flux measurements corrected to the top of the atmosphere on the assumption of an incident isotropic radiation. The dots and crosses represent the results obtained from opening angles and relative scattering measurements normalized to the flux measurements at 3 Bev. The proton spectrum is obtained from the spectrum of Winckler. The solid curves drawn for the heavy nuclei are represented by $N(\epsilon)=K/(1+\epsilon)^{1.35}$ and for the protons by $N(\epsilon)=4000/(1+\epsilon)^{1.07}$, where ϵ is kinetic energy in Bev per nucleon.

A velocity spectrum independent of atomic number would be in agreement with the assumption that the particles are accelerated by some electromagnetic mechanism in which most of the energy is given to the particles after they have traversed several μ g/cm^2 of matter and attained identical charge to mass ratios. At the same time the amount of matter traversed before completing the acceleration should not be large enough to make nuclear collisions probable, because if the acceleration were terminated by a nuclear collision, the largest nuclei would spend the shortest time in the acceleration process and should therefore have a spectrum which falls off faster than that of smaller nuclei. Such assumptions could account for, but do not necessarily follow, from our results.

CHAPTER V. NUCLEAR COLLISIONS OF HEAVY PRIMARIES

In the course of the work described in the previous chapters nearly 1000 particles were traced into the brass stack and their nuclear collisions were observed as described in Chapter II. In terms of g/cm^2 the stack was composed of 88 percent brass, 10.7 percent glass, and 1.3 percent emulsion. Since the mean free path of primaries in glass was determined previously,[3] the mean free path in brass can be obtained.

The collision mean free path was determined both in the Minnesota and White Sands stack. A total of 305 collisions was observed. The results for corresponding charge groups were the same within the statistical error. Since more than half of the particles in the Minnesota stack have energies below 1.5 Bev/nucleon, while all of the particles in the White Sands stack have energies above 1.5 Bev/nucleon, the results show that, as expected, the cross section for nuclear collisions does not depend strongly on particle energy.

A mean free path in brass has also been obtained for α-particles of kinetic energy above 10 Bev by tracing the shower particles described in Chapter I.

The results obtained in brass as well as our previous results in glass are given in Fig. 13. The experimental points are much higher that the dotted curves which represent the values predicted, on the assumption that the collision cross section is equal to the geometric cross section. The data for both materials are, however, well represented by the solid curves which correspond to the cross section:

$$\sigma=\pi(R_1+R_2-2\Delta R)^2, \qquad (11)$$

where the subscripts refer to the target and projectile,

$$R=1.45\times10^{-13}A^{\frac{1}{3}} \text{ cm}, \quad \Delta R=1.0\times10^{-13} \text{ cm}.$$

The validity of this relation, which had been suggested by previous data,[2] has now been tested for absorbers whose atomic weight lies between that of air and brass and for incident nuclei from helium to iron.

[21] P. Freier *et al.*, Phys. Rev. 84, 384 (1951).
[22] A. D. Dainton *et al.*, private communication.

CHAPTER VI. FLUX AND ENERGY DETERMINATIONS IN THE RANGE OF $10^{11} \leq \varepsilon \leq 10^{14}$ EV

When scanning a plate well imbedded in the brass stack, one frequently encounters large numbers of parallel minimum ionization tracks, often grouped into several distinct cores. When following these showers in the downward direction the multiplicity of tracks increases rapidly. In most cases it reaches a maximum value and then decreases again. If followed into the upper hemisphere, one finally reaches the plate where the divergence of tracks permits constructing the location of the shower origin in the brass plate above. If this origin lies close to the emulsion, it is at times possible to observe the shower of the charged mesons before the γ-rays produced by neutral mesons have been converted. The latter are near the origin of the showers, recognizable by the close doublets which they produce.

Apart from giving information on the multiplicity, lifetime, energy distribution, and angular distribution of neutral mesons, on the multiplicity and angular distribution of charged mesons, and on the multiplication of the soft component, these showers permit the determination of the primary flux of protons and α-particles in the energy region between 10^{11} and 10^{13} ev.

We have at present 35 of such showers whose energy exceeds 10^{11} ev. Several of such events exceed 10^{12} ev and one exceeds 10^{13} ev.

The analysis of these events has not been completed. Of 9 showers of energy above 10^{11} whose primaries have been identified, four were probably produced by γ-rays entering from outside, four were produced in the stack by singly charged particles and one was produced by a primary α-particle.

The brass stack proves to be a very efficient detector for soft showers of energy above 10^{11} ev and for the primaries initiating these events. It should therefore be possible to extend the energy spectrum for protons and α-particles to energies above 10^{13} ev.

We wish to express our gratitude to Bausch and Lomb Optical Company, who constructed for us a special microscope which was indispensable for some of the measurements described here.

We are also indebted to the staff of General Mills Aeronautical Laboratory and especially to Mr. A. T. Bauman, who made the balloon flights.

The largest and hardest part of the scanning work was done by Mrs. Katherine Reynolds, whose contribution was invaluable. We are also indebted to Mr. N. Wilson, Mrs. E. Woodruff, and Miss H. Pedell, who assisted in the scanning.

We wish to thank the Office of Naval Research for arranging the balloon flights.

APPENDIX I. STATISTICAL TREATMENT OF CENTER OF GRAVITY AND PLATE SPACING CORRECTIONS

In performing measurements on showers it was usually not possible to determine experimentally the axis of the shower. In these cases the "center of gravity" of the particles was used as an axis. Section A relates the opening angle measured relative to the center of gravity to the true opening angle. Section B relates the scattering measured relative to the center of gravity to the true scattering. Section C concerns the more general problem of removing simulated scattering caused by relative rotation, tilting and uneven spacing of the plates. We derive the relation which was used to correct for uneven plate spacing since this was the only cause of error large enough to affect the measurements in the stack used. The identical method can be used to derive the more general relation. At a distance R from the origin of the shower we construct a plane perpendicular to the shower axis. We choose as the origin of our coordinate system in this plane its intersection with the shower axis.

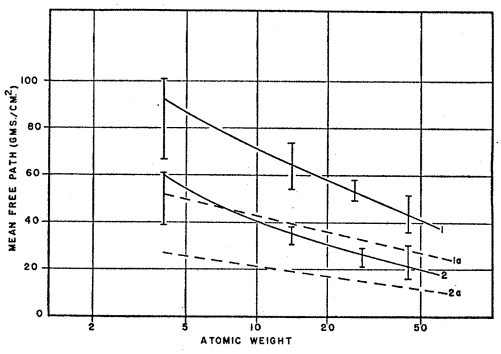

FIG. 13. Mean free paths in brass (1) and glass (2) for particles of various atomic weights. The solid curves represent the empirical relation of Eq. (11), ($\Delta R = 1.0 \times 10^{-13}$ cm) and the dotted curves are the corresponding geometric mean free paths ($\Delta R = 0$).

We define the following symbols:

$X_{i,\lambda}(\lambda = 1,2)$ are the Cartesian coordinates of the intersection of the ith track with the plane.

$\theta_i = (1/R)(\Sigma_\lambda X_{i,\lambda}^2)^{\frac{1}{2}}$ is the angle of the ith track with the shower axis.

$X_\lambda = (1/n)\Sigma_i X_{i,\lambda}$ are the coordinates of the intersection of the center of gravity axis with the plane.

$x_{i,\lambda} = X_{i,\lambda} - X_\lambda$ are the coordinates of the intersection in the plane of the ith track measured with respect to the intersection of the center of gravity axis.

$\phi_i = (1/R)(\Sigma_i x_{i,\lambda}^2)^{\frac{1}{2}}$ is the angle between the ith track and the center of gravity axis.

$S_{i,\lambda}^T$ is the true scattering of the ith track projected on the λ-axis.

$S_{i,\lambda}$ is the measured scattering or the second differences in the position of the ith track with respect to the center of gravity of the shower.

n is the total number of shower particles.

Section A

The mean square opening angle of the shower tracks with respect to the shower axis ($\langle\theta^2\rangle$), can be expressed in terms of the measurable mean square opening angle of the tracks with respect to the center of gravity of the shower ($\langle\phi^2\rangle$).

In terms of the symbols defined above we have:

$$x_{i,\lambda}^2 = (X_{i,\lambda} - X_\lambda)^2 = [X_{i,\lambda} - (1/n)\sum_j X_{j,\lambda}]^2,$$

$$\sum_i x_{i,\lambda}^2 = \sum_i X_{i,\lambda}^2 - \frac{2}{n}\sum_i X_{i,\lambda}^2 + \frac{1}{n}\sum_i X_{i,\lambda}^2 = \frac{n-1}{n}\sum_i X_{i,\lambda}^2,$$

since for tracks randomly distributed in azimuth

$$\sum_{i,j} X_{i,\lambda} X_{j,\lambda} = 0 \text{ for } i \neq j.$$

Using the definitions given above we therefore obtain

$$(1/n)\sum_i \phi_i^2 = [(n-1)/n^2]\sum_i \theta_i^2 \quad \text{or} \quad \langle\phi^2\rangle = [(n-1)/n]\langle\theta^2\rangle.$$

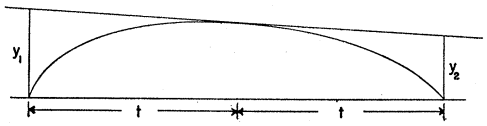

FIG. 14. Parameters used in determining the sagitta scattering constant.

Section B

A correction must be applied to the scattering data since the measurements are made with respect to the center of gravity. Assume for the moment that there is a rigid reference line travelling through the stack of plates and that the displacements with respect to it are $X_{i,\lambda}$ for the first plate, $X_{i,\lambda}'$ for the second plate, and $X_{i,\lambda}''$ for the third plate. The second difference of the displacements from the center of gravity is

$$S_{i,\lambda}=(X_{i,\lambda}-2X_{i,\lambda}'+X_{i,\lambda}'')+(2\sum_j X_{j,\lambda}'-\sum_j X_{j,\lambda}-\sum_j X_{j,\lambda}'')/n.$$

The true scattering is

$$S_{i,\lambda}{}^T=(X_{i,\lambda}-2X_{i,\lambda}'+X_{i,\lambda}'').$$

Therefore

$$S_{i,\lambda}=S_{i,\lambda}{}^T-(1/n)\sum_j S_{j,\lambda}{}^T.$$

Squaring and taking the average (the procedure is identical to that of A)

$$\langle S^2\rangle=[(n-1)/n]\langle(S^T)^2\rangle,$$

where the average of the cross terms is zero since there is equal chance for $S_{i,\lambda}{}^T$ to be positive or negative.

Section C

A statistical correction which removes the simulated scattering due to plate spacing differences is possible because the plate spacing differences change the distance between tracks by the same percentage. The process consists of minimizing the measured scattering by hypothetically changing the plate separation and then adding back the amount of true scattering removed in this process. The derivation is as follows: The measured scattering is

$$S_{i,\lambda}=S_{i,\lambda}{}^T-(1/n)\sum_j S_{j,\lambda}{}^T-ax_{i,\lambda},$$

where a is a correction term which compensates for the difference in plate spacing since the simulated scattering due to plate spacing differences is proportional to the projected opening angles of the tracks.

We define:

$$\Omega_{i,\lambda}=S_{i,\lambda}-a'x_{i,\lambda},$$

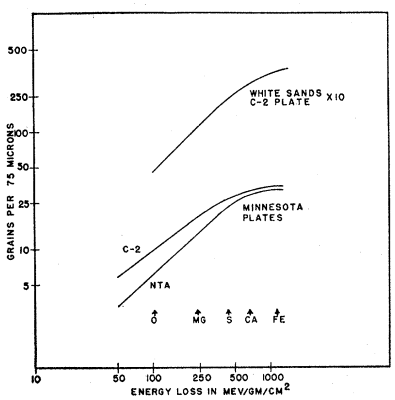

FIG. 15. Calibration curves for underdeveloped C-2 and NTA emulsions.

where a' has such a value that $\sum_{i,\lambda}\Omega_{i,\lambda}{}^2$ is a minimum. The value of a' is then

$$a'=\sum_{i,\lambda}x_{i,\lambda}S_{i,\lambda}/\sum_{i,\lambda}x_{i,\lambda}{}^2.$$

With the above definitions

$$\Omega_{i,\lambda}=S_{i,\lambda}{}^T-\frac{1}{n}\sum_j S_{j,\lambda}{}^T-x_{i,\lambda}\sum_{j,\mu}x_{j,\mu}S_{j,\mu}{}^T/\sum_{j,\mu}x_{j,\mu}{}^2.$$

Since $\sum_j x_{j,\lambda}=0$ by definition, we find on squaring and taking the average that

$$\sum_{i,\lambda}\Omega_{i,\lambda}{}^2=(2n-3)\langle(S^T)^2\rangle$$

or

$$\langle\Omega^2\rangle=[(2n-3)/2n]\langle(S^T)^2\rangle.$$

APPENDIX II. SCATTERING CONSTANT

In order to determine the scattering constant we note that (a) the measurement is a second difference measurement (sagitta type), and (b) the scattering takes place across cells composed of layers of glass, brass, emulsion, and air.

It can be shown that the sagitta scattering constant is simply related in the Gaussian approximation to the Williams-Molière theory of scattering between successive tangents in a homogeneous medium. In Fig. 14 the second difference is $S=Y_1+Y_2$, where Y_1 and Y_2 are the distances of the track from the tangent to the track at the center of the cell and $\langle S^2\rangle=\langle Y_1{}^2\rangle+\langle Y_2{}^2\rangle$. The formula for Y^2 is given by $t^3\alpha_0{}^2/3$, where $\alpha_0{}^2$ is the Williams scattering parameter for a unit cell length. In an inhomogeneous medium

$$\langle Y^2\rangle=\tfrac{1}{3}t^3\{\alpha_1{}^2[1-(1-k_1)^3]+\alpha_2{}^2[(1-k_1)^3-(1-k_1-k_2)^3]+\cdots$$
$$+\cdots\alpha_m{}^2(1-\sum_{i=1}^{m-1}k_i)^3\},$$

where $\alpha_m{}^2$ is the scattering parameter for the various materials in order of succession from the center of the cell and k_i is the fraction of the cell taken up by each material. Using these expressions for the brass stack the scattering relations for particles with $Z/m=\frac{1}{2}$ become

$$\langle S^2\rangle^{\frac{1}{2}}=14.5t^{\frac{3}{2}}/p\beta \text{ for a 1 plate spacing,}$$
$$\langle S^2\rangle^{\frac{1}{2}}=15.4t^{\frac{3}{2}}/p\beta \text{ for a 2 plate spacing,}$$

where S is in microns, t is in units of 5000 microns, $\beta=v/c$, and p is the momentum in units of the proton rest mass. For the particular cell lengths chosen, the values of α^2 have the ratios

$$\text{brass:emulsion:glass}=9.7:4.6:1.$$

APPENDIX III. CHARGE CALIBRATION

At northern latitudes a large fraction of the particles are slow (nonrelativistic). Therefore track identification must be based on simultaneous ionization and range measurements.

The NTB-3 and G-5 emulsions were developed with the usual temperature method. The C-2 and NTA emulsions were heavily underdeveloped using the usual temperature method with D-25 as the developer. The warm stage of the process occurred at 15°C for 15 minutes.

The calibration of the insensitive plates was established in the following manner: (a) In the insensitive plates, tracks of α-particles emitted from stars were observed and grain counted at known distances from the end of their range. To assure that these particles were alphas, the end of their ranges were compared with the alphas from thorium stars. This calibrated a range of ionization from 60 to 500 times minimum. (b) The heaviest ionizing tracks occurring with reasonable frequency and penetrating the stack are due to iron nuclei. This fact was used to establish the high ionization end of the calibration curve for the insensitive plates.

Thus a complete calibration for the insensitive plates was obtained from an ionization corresponding to relativistic iron to one

corresponding to relativistic oxygen. The δ-ray calibration was established as follows:

(a) High energy α-particles (approximately 20 Bev per nucleon) resulting from a C-collision, were δ-ray counted. Minimum ionization tracks were also δ-ray counted. Since for relativistic particles:

$$\delta_Z = Z^2 a + b,$$

where "a" is a constant and "b" the δ-ray density due to random electrons, both "a" and "b" can be determined.

(b) Because of the difficulty in maintaining the same criterion for δ-ray counting when counting a track of minimum ionization the method described above is not extremely reliable. Therefore particles which were identified as oxygen in the insensitive plates were δ-ray counted in the sensitive plates. The results were consistent with the δ-ray calibration from relativistic protons and α-particles.

Using this calibration we obtain in the primary flux a strong peak corresponding to the CNO group and very few particles of charge $2<Z<6$ in agreement with our previous results.[3]

The calibration curve for the C-2 and NTA emulsions is shown in Fig. 15. It will be noted that the curves reach saturation at very low grain densities. We presume this could be avoided by using less sensitive emulsions and less underdevelopment. For steep heavy tracks δ-ray counts became unreliable and grain counts were used to determine charge.

Corresponding results were obtained with the White Sands charge calibration.

PHYSICAL REVIEW VOLUME 85, NUMBER 2 JANUARY 15, 1952

The Variation of Intensity of Fast Cosmic-Ray Neutrons with Altitude

L. F. CURTISS*
National Bureau of Standards, Washington, D. C.

AND

P. S. GILL
Department of Physics, Aligarh University, Aligarh, India

(Received August 29, 1951)

Using BF_3 proportional counters, containing boron enriched in B^{10}, imbedded in a paraffin block 15×15×17 inches, as a moderator of fast neutrons, the intensity of such neutrons generated in the atmosphere by cosmic rays has been measured at a number of altitudes between 5000 and 13,000 feet above sea level. These locations were all along the same geomagnetic latitude of 20° 32′ N in Kashmir. The intensity thus measured was found to increase approximately in an exponential manner with decreasing atmospheric pressure under the conditions of the experiments, in general agreement with observations made by other investigators in the free atmosphere, giving an attenuation length in the atmosphere of 128 g/cm².

I. INTRODUCTION

CONSIDERABLE interest has been shown in the last decade in the neutron component of cosmic radiation with attention focused chiefly on the slow neutrons in the atmosphere. The slow neutrons offer the advantage of detection by relatively simple means, such as BF_3 counter tubes, which makes possible the use of equipment of light weight suitable even for free balloon flights. This accounts in part for the numerous investigations of their variation in intensity with altitude.

Detectors of fast neutrons, on the other hand, are usually heavy and bulky, since to date the most satisfactory method of detecting these neutrons is to moderate them in some medium, such as paraffin, and then to detect them as slow neutrons with BF_3 counters imbedded in the moderator. Such devices cannot be carried aloft readily by balloons. Consequently about the only convenient way of making measurements of fast neutrons generated in the atmosphere at various levels is either to transport the equipment to various heights on the surface of the earth or to use airplanes. Observations with airplanes suffer from an inability to maintain even an approximately constant position laterally and vertically for the relatively long time required to obtain measurements of a statistical accuracy of the order of one percent. Also the use of planes for this purpose is expensive. Since fast neutrons are presumably a direct product of that type of interaction between the cosmic radiation and atomic nuclei which leads to nuclear disintegration, it is reasonable to suppose that the study of fast neutrons in the atmosphere would give more direct information regarding the nature of this process than is obtained from data regarding slow neutrons.

These considerations led the authors to attempt to obtain information regarding the variation of intensity of fast neutrons in the atmosphere over a limited range of altitudes at some elevated location on the surface of the earth. The region selected for these trials is in Kashmir where altitudes between 5000 and 13,000 feet are accessible lying along the same geomagnetic latitude 20° 32′ N. Also adequate manpower at low cost is available there to carry the relatively heavy equipment up over the snow fields and rough terrain in the steep

* Fulbright research scholar assigned to Aligarh University, Aligarh, India.

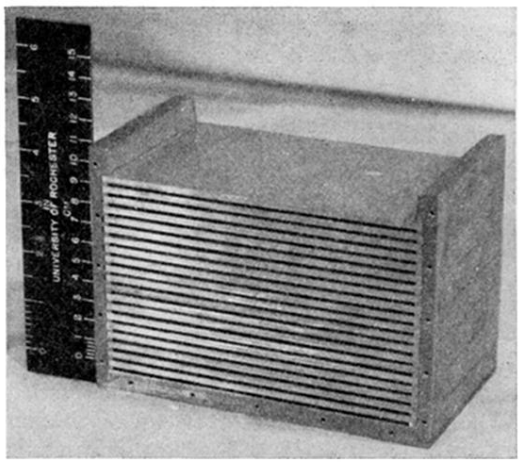

FIG. 3. Brass box used for exposing plates.

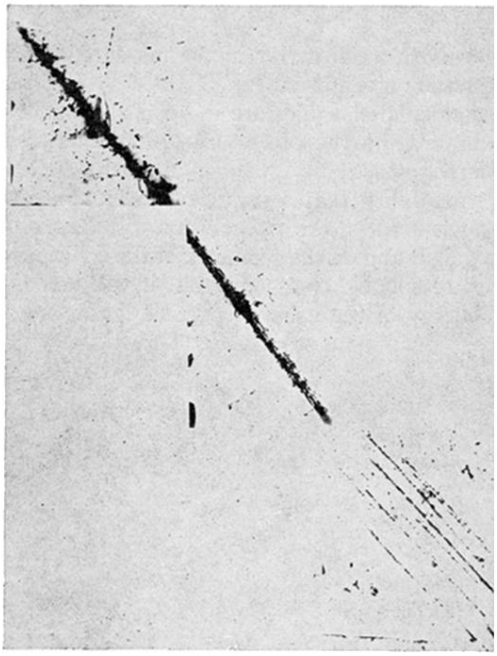

FIG. 4. *C*-collision: A primary Fe nucleus with a total energy of 2×10^{12} ev strikes a nucleus of the emulsion and breaks up into a highly collimated shower of 6 α-particles, a Be nucleus, and several protons. The first plate shows the incident nucleus before breakup. The second plate (4.6 mm from the first) shows the collimated shower shortly after breakup. The third plate (6.8 mm from the second) shows the separate components of the shower. The total spread in plate 3 is 30μ.